Journal of Applied Fluid Mechanics, Vol. 18, No. 2, pp. 363-373, 2025.
Available online at www.jafmonline.net, ISSN 1735-3572, EISSN 1735-3645.
https://doi.org/10.47176/jafm.18.2.2844

Improving Wind Turbine Power with Boundary Layer Suction

S. Sadi[1], M. R. Asayesh[2] and S. A. Moussavi[3†]

[1] *Imam Hossein Comprehensive University, Tehran, Iran*
[2] *Department of Energy Engineering, Azad Islamic University, Tehran, Iran*
[3] *Niroo Research Institute, Tehran, Iran*

†*Corresponding Author Email: samoussavi@nri.ac.ir*

ABSTRACT

Given the vast global capacity of wind turbines, even minor enhancements in their overall performance can substantially increase energy production. To achieve this, several techniques have been developed and implemented commercially to create advanced blades with improved efficiency. However, the fixed aerodynamic shape of these blades imposes certain constraints. This study conducts a numerical analysis of a 660 kW wind turbine, revealing that under specific operating conditions, the blades experience off-design conditions, leading to performance degradation. Simulations indicate that because the blades are designed for a single operating point, flow separation occurs on some sections of the blade surface in other situations. Further investigation demonstrates that the fixed geometry of the blades hinders the flow's ability to adapt to their shape. To address this challenge, the method of boundary layer suction is proposed. Results indicate that by applying an appropriate level of suction intensity, the aerodynamic performance of the rotor can be enhanced by up to 8% under the specified working conditions by facilitating flow reattachment at the inboard section.

Article History

Received May 11, 2024
Revised September 1, 2024
Accepted September 5, 2024
Available online December 4, 2024

Keywords:

Wind Turbine
Boundary layer suction
Flow separation
Aerodynamics
Performance

1. INTRODUCTION

The share of wind in the energy mix of the world has experienced impressive growth over recent decades. This trend has been amplified in periods of uncertainty in the price of oil or other energy sources. Developing investment in this field has led to increasing wind turbine sizes up to 14MW per machine. To achieve this state, manufacturing and material technologies seem to have the most important role. Otherwise, no breakthrough can be observed in the aerodynamic design of recent blades. It seems that the current blade design has reached a mature state. Accordingly, we expect the entrance of new solutions for the remaining issues.

An important limitation in the current design is the invariableness of blade twist distribution. It can be rapidly concluded that this geometry may not be suitable for all working conditions in which the blade is exposed. To address the issue, the design steps of the blade should be examined.

The blade design procedure starts with assuming some parameters such as rated wind velocity, design tip speed ratio (TSR), and airfoil type that are considered fixed throughout the steps and cannot be changed later. Tip Speed Ratio denoted as TSR is the ratio of blade linear tip speed and wind speed. This is one of the crucial parameters in designing a wind turbine blade which mostly affects the blade twist angle distribution. By implementing BEM (blade element momentum) theory, all other geometric dimensions of the blade including length, chord, and twist distribution can be calculated and optimized. Thus, it can be directly concluded that these geometric parameters are only optimal for a unique condition (design TSR). In other words, if the blade is not operating exactly on this point, it will be off-design and some efficiency loss will be inevitable.

Since manufacturing morphing blades (with variable geometry) is not yet possible, implementation of flow rectification methods which are well known in the aerodynamic industry may be suitable. Their goal is to alter the flow on the airfoil and obtain some new behavior from the same geometry. This can result in lower drag, less noise, improved lift, and higher stall angle. For this purpose, several solutions have been investigated in the literature. A major group of them deals with flow separation as the most important challenge in aerodynamics. Flow separation occurs when the flow can no longer follow the wall profile and deviates from it. When passing over a bent surface or diverging passage,

the flow near the surface needs to decelerate and change its direction. Upon reduction of the speed, pressure will increase along the direction of flow referred to as an unfavorable pressure gradient. In sharp surface curvatures, this process continues until the flow energy near the surface is completely depleted and the flow stalls. The fluid in the upper layers tends to continue its path and thus the flow separates from the surface. Generally, the techniques addressing this issue can be classified into three main mechanisms. The first tries to reenergize the dead boundary layer and force it to continue its path. This energy can be supplied from the far field flow through a mixing mechanism or by external sources such as electricity.

Vortex generators may be the simplest mechanism in this category. The use of vortex generators on a stall-regulated wind turbine is reported by Griffin (1996). The technique is still discussed in newer papers such as the work of Zhu et al. (2019) and Mereu et al. (2019). The first working prototype was installed on the 2.5MW MOD-II wind turbine in 1982 (Spera, 2009). The commercial production and installation of this device are now accessible in the market for which up to 3% increase in Annual Energy Production (AEP) has been reported.

The mixing required for energy transfer may be generated by the use of surface dimples, such as the work of Mahboub et al. (2022) and Sedighi et al. (2020), altering surface roughness (Ozkan and Erkan, 2022), additional bodies at the leading edge such as tubercles (Supreeth et al., 2020) or cylinders (Shi et al., 2019) or ribs (Jacob & Santhanakrishnan, 2005). Another method welcomed in the literature is the plasma actuator. The method is easy to implement with low energy consumption and some limitations. The effect of such a mechanism on a wind turbine is investigated in the work of Jukes (2015) and Guoqiang and Shihe (2020).

The second group includes methods based on variations of pressure gradient through profile modification. Since adverse pressure gradient is the main cause of flow separation, here the body profile is being changed to attain a more favorable flow. In the industry, this has been achieved using trailing edge flaps (Huang et al., 2023) and gurney flaps (Mayda et al., 2005). Recently smart rotor blades have been also introduced with deformable trailing edges as studied by Basualdo (2005), Barlas and Van Kuik (2007), van Wingerden (2008), and Pechlivanoglou (2010). The effect of deformable leading edge is also studied in the work of Pechlivanoglou (2013) but it does not seem to be very promising.

The last group which is the subject of this work relies on the boundary layer suction (BLS) method. By applying a suction through a slot made on the suction side of an airfoil and located at the onset of flow separation, the stalled or low energy fluid in the boundary layer which is distancing between the surface and main flow, can be extracted and replaced with a more energetic flow. Indeed, with this initiative, the flow can be reattached. Several experimental and numerical works investigating the effect of suction on NACA airfoils can be found in the literature. Karim and Acharya (1994) and Alfrefai and Acharya (1996) experimented the effect of suction on the leading edge of NACA0012 at Re=1e5. With the suction area located within 2-5% of the chord length, they reported that the separation and the dynamic stall can be suppressed. Wang (1995) studied the suction on the leading edge section to control the flow separation and dynamic stall of a NACA0012 airfoil by numerical methods. In his work, the suction slot was located at 20% of the chord length. He showed when the suction is applied at the right position, the flow separation and dynamic stall can effectively be suppressed, accompanied by an increase in lift. Yousefi et al. (2012) studied the aerodynamic behavior of a NACA0012 airfoil under different angles of attack. They found that when the suction slot is located at 10% of chord length with a suction coefficient of 0.5, the airfoil demonstrates optimum aerodynamic performance, with the lift coefficient growing by about 45% and the drag dropping by 29% and its angle of stall shifting from 14° to 20°. Ma and Xu (2023) studied the effect of simultaneous injection and suction of flow on the S809 airfoil. Compared with the conventional airfoil, the designed conformal slot airfoil has three advantages: eliminating the performance loss when the jet is off, saving jet energy when suppressing the flow separation, and improving the power generation of wind turbines at low wind speeds. However, they did not directly study its effect on wind turbine performance. Arnold et al (2018) studied this concept for noise reduction purposes on NREL 5MW wind turbine. Moussavi and Ghaznavi (2021) have suggested its implementation for performance improvement of a 2MW wind turbine and demonstrated up to 8% improvement in power production under certain conditions.

As can be observed, the literature provides few works about the use or study of boundary layer suction on wind turbines. The technique is also not commercialized yet for wind turbines. So, we believe that the implementation of the boundary layer suction method can become interesting for the wind industry if it is sufficiently investigated in academic literature. Here we intend to numerically examine the effect of installing a boundary layer suction on a 660kW wind turbine that is still operational in the country (Fig. 1). Our selection is backed up by the availability of operational and geometric data of that turbine. To this end, the numerical model of the blade is

Fig. 1 wind turbine under study

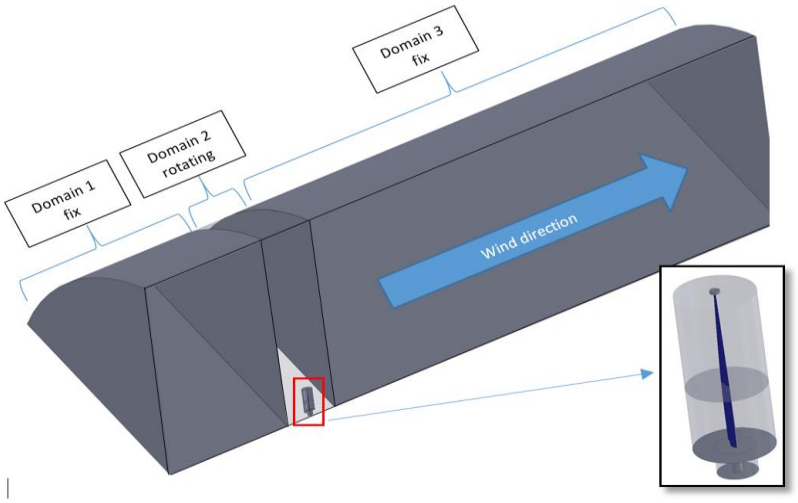

Fig. 2 Cross section of the computation domain around the turbine

Table 1 wind turbine general specifications

Rated power	660 kW
Rotor diameter	47 m
Hub diameter	2.2m
Blade length	22.4m
Max cord	2088 mm
Airfoil type	FFA W3/ NACA63
Blade root diameter	990mm
Power regulation	Pitch system
Hub height	50 m
Rated wind speed	12 m/s
Rated rotor speed	28.5 rpm
Max power coefficient	0.47

generated and its original aerodynamic performance is evaluated using CFD method under various working conditions. Streamlines are then carefully examined in different spans of the blade and the undesirable flow pattern is revealed. To further investigate the feasibility of the proposed method, structural analysis of the blade is performed and some modifications are made in blade geometry accordingly. Finally, turbine performance after implementation of the suggested system is re-evaluated and discussed. We hope that considering the results of this work, the concept can be executed on the mentioned turbine in the future.

2. NUMERICAL MODEL

The wind turbine's key specifications are outlined in Table 1. This is a 3 bladed horizontal axis wind turbine with automatic pitch and yaw control. The rotor is connected to the generator by a gearbox. Since the manufacturing plant is still active, the 3D CAD model of the blade was generated according to data obtained from documents (Fig. 2). To study the flow around the blade, the numerical domain was generated as a 120 degree section of a long cylinder.

The cylindrical domain extends 3 rotor diameters upwind, 8 diameters downwind, and 4 diameters radially. This domain is divided into three volumes, with the central volume containing the blade rotating at a pre-defined speed. To enable flexible blade pitch angle adjustments without re-meshing, the blade is positioned within a separate cylindrical sub-domain, connected to the outer domain through an interface (domain 2). Given the critical nature of the flow around the blade, a structured C-grid with a refined boundary layer was generated using the blocking method within this sub-domain. This grid features a first layer thickness of approximately 8 microns on the blade surface, with a 20% growth rate to achieve a maximum y^+ of about 7 at the tip and 3 near the root (Fig. 3). Unstructured tetrahedral and hexahedral elements are employed in the other domains, with increasing element size towards the domain boundaries.

To simulate the airflow, the steady-state Reynolds-Averaged Navier-Stokes (RANS) equations were solved using ANSYS CFX, employing the k-ω SST turbulence model (Rezaeiha et al., 2019; Maali Amiri et al., 2020) and assuming isothermal incompressible air as the working fluid. As shown in Fig.2, the simulation setup included a velocity inlet boundary condition on face 1 representing

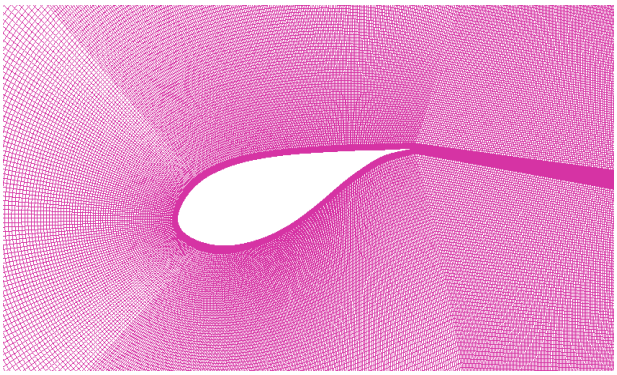

Fig. 3 Grid around the blade at root section

Table 2 Results of mesh independency analysis

Case number	Elements count	Number of layers near blade surface	Power (kW)	Thrust (kN)
1	18.5E6	5	581	79.2
2	21E6	10	640	83.5
3	23E6	15	652	84.8
4	28E6	20	670	87.1
5	31E6	25	678	88

the free stream entering the domain, a pressure outlet condition on face 3 with zero relative static pressure, and rotational periodic conditions on the lateral boundaries (face 4). A far-field velocity vector aligned with the inlet direction was specified on the upper boundary (face 2). The blade surface was assumed as a no-slip wall.

To ensure the accuracy of our simulation results, a mesh independence analysis was conducted. Turbine power and thrust were calculated under rated conditions using five different mesh densities, primarily varying the mesh around the blade. As shown in Table 2, the last two mesh configurations resulted in a difference of only 1% in turbine performance. Therefore, mesh number 4 was chosen for this study, featuring 408 nodes chordwise and 400 nodes spanwise along the blade.

To validate numerical results, they were compared to operational data from the actual wind turbine. Power, wind speed, and rotor speed were extracted from the turbine's central control system, which continuously monitors atmospheric and operational conditions. The wind turbine utilizes a cup anemometer (or, more recently, lidars) mounted on the nacelle to measure wind speed, provide data to the control system, and ensure safety. Turbine power is measured by monitoring the generator's current and voltage through the converter system. The manufacturer reports a generator efficiency of 98%, allowing us to easily calculate the mechanical power at the main shaft.

The turbine's central control system logs various operational parameters, including time, power, wind speed, and shaft speed, at 10-second intervals. Due to the inherently variable nature of wind, the turbine operates under constantly changing conditions rather than a steady state. For this study, time, power, wind speed, and shaft speed were extracted from the log file. Then data was averaged over one-minute intervals, effectively eliminating temporal variations. These averaged data points were subsequently grouped into wind speed bins with a width of ±0.25 m/s. Finally, the data within each bin were averaged again and the results presented in

Figure 4. Our analysis reveals that the numerical results closely match the experimental data for zero pitch angles. The maximum error observed is approximately 10 kW at a wind speed of 9 m/s, corresponding to a relative error of 2.5%.

This trend remains valid until wind speed of 12m/s which is the rated wind speed at which the nominal power is extracted. Beyond this speed, the power regulation system comes into operation and gradually changes the blade pitch angle to keep the energy capture constant. To demonstrate this action, curves for 5 and 9-degree pitch

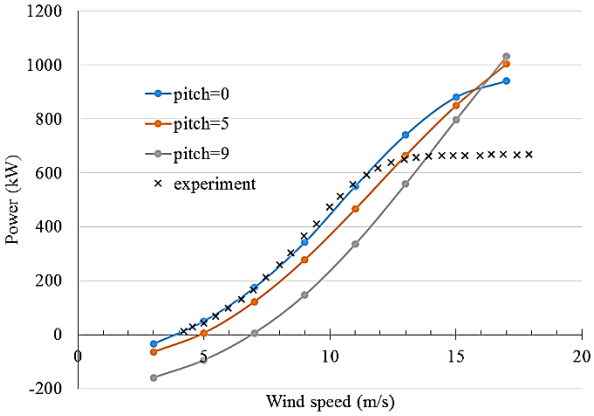

Fig. 4 Experimental vs numerical power curve

angles have also been plotted. From the operation log of the turbine, it was read that at a wind speed of 13m/s, the pitch angle is about 5 degrees. It can be observed that at 13m/s the corresponding curve, reaches the rated power too, thus validating the second curve. The same strategy may be followed for the third pitch angle.

3. ACTUAL FLOW FIELD

In the first step, it is necessary to analyze the operational parameters of the wind turbine. In analyzing the performance of a wind turbine, two dimensionless parameters are commonly used and defined as below:

$$TSR = \frac{R\omega}{V_{wind}} \quad (1)$$

$$C_p = \frac{P}{0.5\,\rho A V_{wind}^3} \quad (2)$$

Here TSR is the tip speed ratio, C_p denotes the power coefficient, R [m] represents rotor radius, ω [rad/s] shows rotor speed, P [W] is output power, A [m^2] shows rotor swept area, V [m/s] stands for velocity, and ρ [kg/m^3] is air stream density.

Two types of curves are common in the industry to describe the performance of a wind turbine:

I. The performance curve in which C_p versus TSR is shown. This curve focuses on blades' aerodynamic performance with the use of dimensionless parameters defined in equations 1 and 2;

II. The power curve which shows the amount of generated power versus wind speed. This curve is plotted by taking into account the entire turbine system, especially the control strategy. In other words, the behavior and the capacity of the turbine as a system is demonstrated.

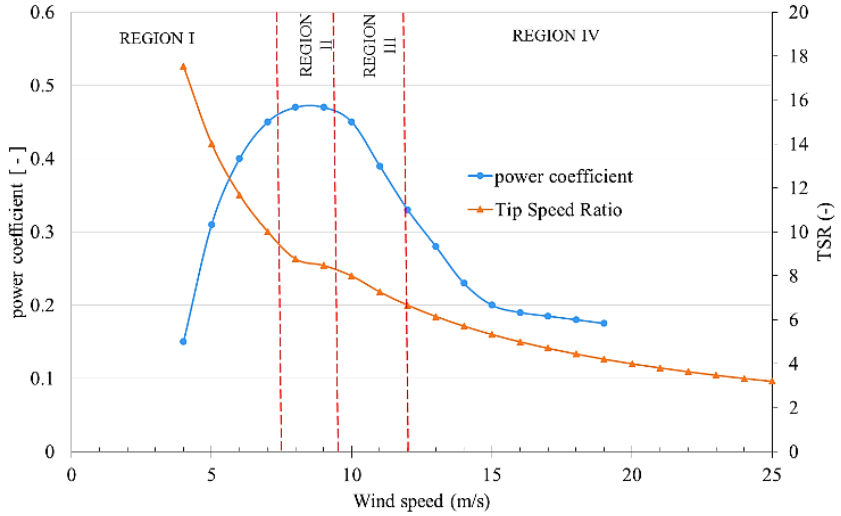

Fig. 5 Operation parameters of the turbine

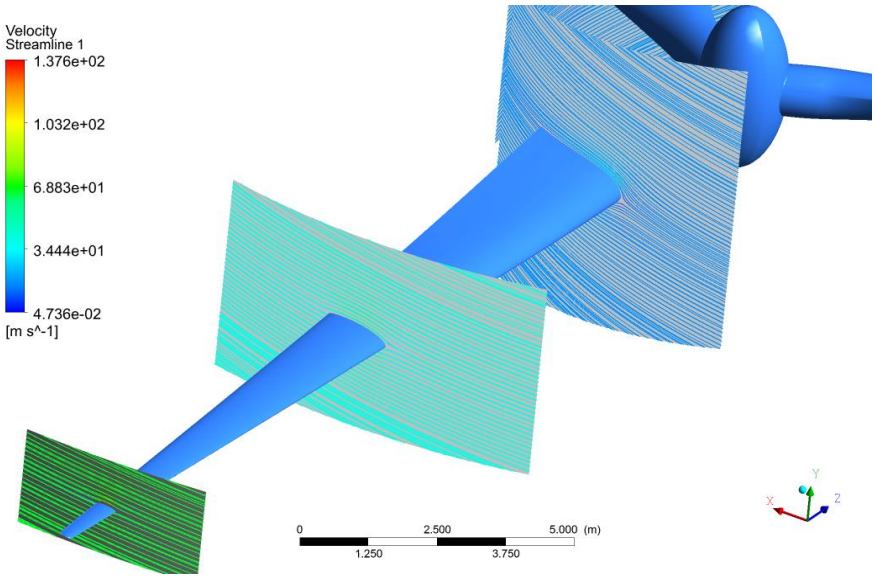

Fig. 6 Streamlines at different sections of the blade for TSR=8.5

The chart provided in Fig.5 is a combination of the above mentioned curves and represents the actual operational TSR of the turbine. The plot is divided into four regions according to wind speed. Region II is equivalent to aerodynamic design conditions of the machine (TSR=8.5) at which the maximum aerodynamic performance (C_p) is reached.

Within this wind speed range (7.5 to 9.5 m/s) the control system comes into action and adjusts the rotor speed by controlling the generator torque to maintain the design TSR. However, this strategy is limited and the rotor speed cannot be reduced too far. The limitation is due to the fact that the delivered electricity needs to comply with the grid code and maintain a steady frequency of 50Hz. Thus, the generator speed cannot be reduced as needed and the design TSR is lost at lower wind speeds (region I) resulting in off design operation of the rotor with lower aerodynamic efficiency. The same occurs when the wind speed is between the design and the rated wind speed (region III). By definition, the rated wind speed (12m/s according to Table 1), is the condition at which wind turbine reaches its nominal power (660kW). Here, the generator has reached its maximum allowed capacity. Hence, with higher wind speed and constant rotor speed, TSR follows a descending trend and recedes from the design state. At higher than rated wind speeds denoted by region IV, the wind power is higher than required. Thus, we do not need to preserve the maximum efficiency. The pitch system comes into operation and enforces a decline in power coefficient to keep the extracted mechanical power constant. In this paper, we have focused on region III, where the pitch control is not active and generator speed cannot be regulated.

To explore the effect of working in off design conditions from an aerodynamic point of view, the flow field should be investigated. Figure 6 displays streamlines around the blade at 3 sections i.e. near root (r=5.5m), mid span (r=12m), and tip (r=23m) at design TSR of 8.5. It can be observed that the flow is completely attached over the entire span and normal conditions dominate as expected.

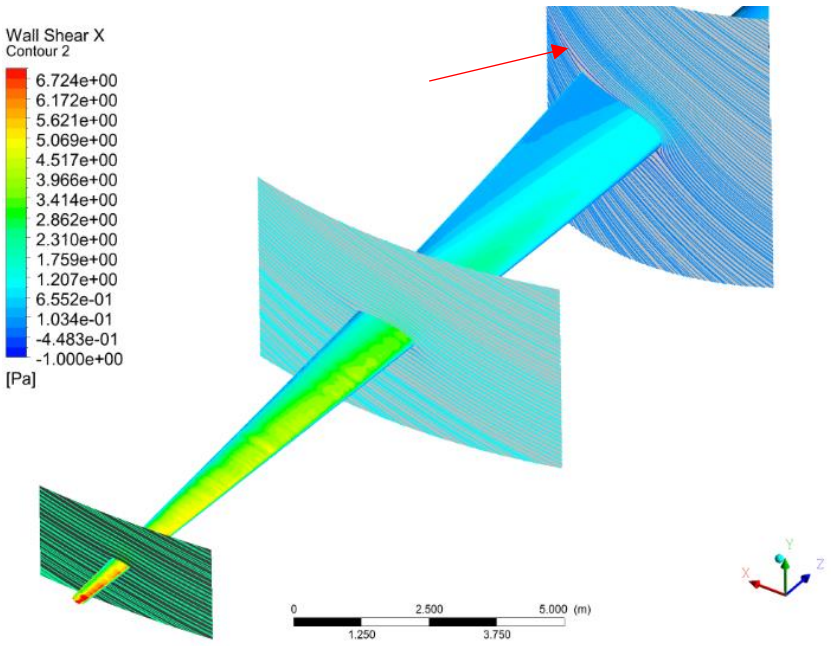

Fig. 7 Streamlines at different sections of the blade at TSR=7

Figure 7 shows streamlines at the same sections at TSR=7 (as in region III of Fig. 5). It can be observed that the flow is no longer attached to the blade and a separation is present, especially at the root. For ease of observation, the contour of wall shear along the x axis is also shown (Fig. 7). The separation occurs where the wall shear changes sign. At the root section, separation can be observed to start at about 50% of cord length. The separation becomes less severe at mid span and vanishes at the tip. This is because the velocity component due to rotation is lower at root section and any variation in normal wind speed can greatly affect the relative wind direction. At the tip, the rotation speed is too high and changes in normal wind speed are less effective.

4. THE SUCTION SYSTEM AND STRUCTURAL CONSIDERATIONS

To rectify the flow under off-design conditions, the boundary layer suction method is proposed. To this end, a slot has to be created on the surface of the blade to extract the stalled fluid. However, care should be taken, because any variation in the blade structure can have an adverse effects on the stress field and blade strength.

Thus, the blade structure has to be taken into account to find regions in which the suction slot can be created.

Examination of the blade structure indicates that it is mainly composed of two parts as depicted in Fig. 8. The first part is the skin which forms the aerodynamic shape with the main task of generating driving forces and moment. These loads are then transferred to the load carrying part, called the spar which has a rectangular cross section and is reinforced with several layers of composite material. The spar is finally lofted into a circular cross section at the root and connected to the hub through bolts. From a manufacturing point of view, the aerodynamic skin is a thin composite layer often with a balsa wood or PVC

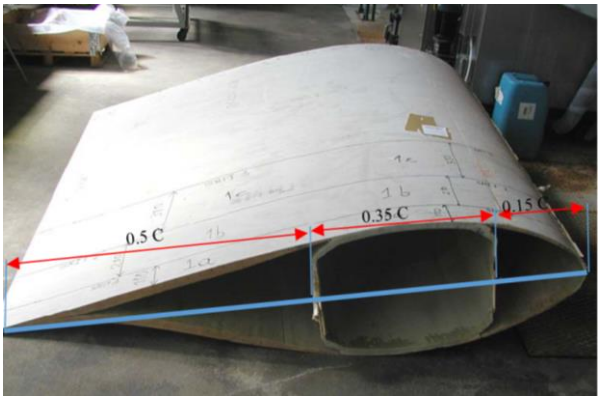

Fig. 8 A blade internal structure and location of reinforcement

core. Thus, it is not considered to carry any load. Since it is not intended to make extensive changes in the blade structure and manufacturing process, it can be concluded that the suction slot cannot be created inside the spar.

Analysis of the blade geometry shows that the spar vertical walls (shear webs) are located at 15 and 50% of the chord in each section. According to the location of flow separation stated in the previous section, 50% of the chord (onset of flow separation) is our first candidate for creating the slot. Basically, it is suggested to apply the suction before the flow separation, but to prevent damage to the spar, the suction slot cannot be placed at the optimal location.

Making a long radial slot on a large-scale wind turbine blade does not seem to be straight forward. According to IEC61400-1 standard, the turbine is exposed to various aerodynamic loading for at least 20 years which makes the blade very sensitive structurally. Thus, to check the applicability of the proposed position of the required slot without altering the blade strength, the structural design of the blade is also examined.

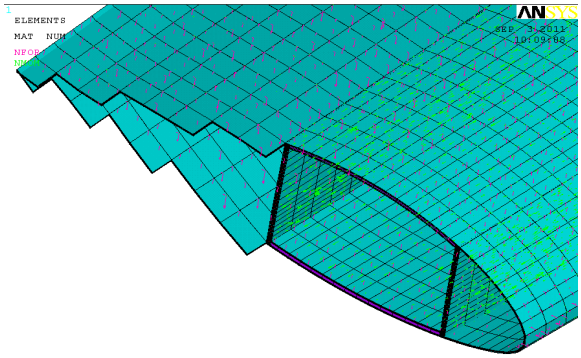

Fig. 9 Numerical model of the blade internal structure

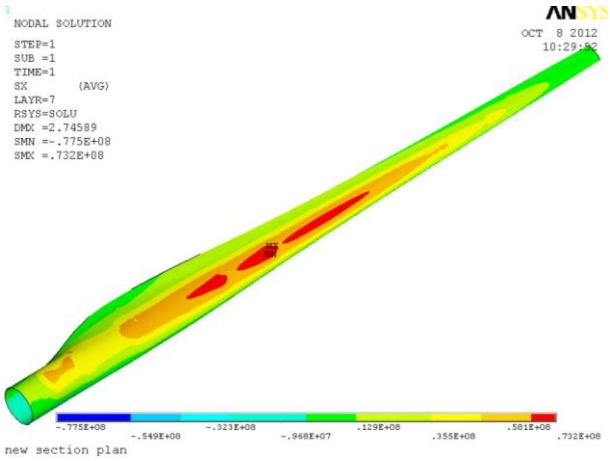

Fig. 10 Lengthwise stress in outermost Uni-Directional layer

To gain an insight into the blade loading, its structural model has been created. The layup of different GFRP (glass fiber reinforced plastic) layers along with their mechanical properties have been taken into consideration through a shell numerical model. The blade has been discretized using 50000 plain shell elements. The cross section of the blade is shown in Fig. 9.

To discover the most sensitive zone of the blade and avoid making holes in it, stress calculations according to loadcase DLC6.1 of IEC61400-1standard has been performed. Loads have been carefully calculated using FAST code developed by NREL and taking into account all dynamic and mechanical properties of the turbine.

They are then transferred to blade surface as discrete point forces. A typical result of blade stress analysis is displayed in Fig. 10. It can be observed that the most critical area is located at the mid span of the blade and completely on the spar cap as expected. Discontinuities in the stress contour are due to layup variations in different blade sections. From this contour, and since making a slot in red zones is forbidden, it can be concluded that the initial proposed location for creating a slot on blade body is suitable.

The size of the slot (width and length) is still a parameter to be determined. According to the flow field

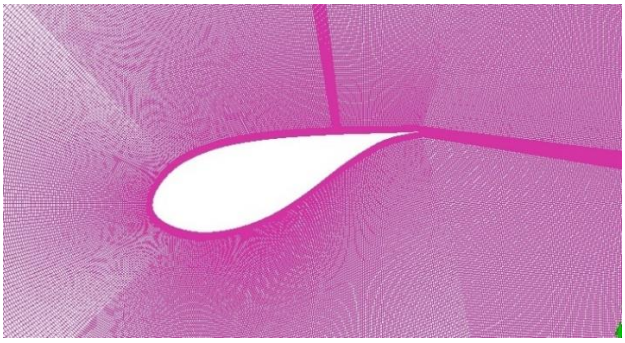

Fig. 11 The modified mesh at the generated new slot

presented in Fig. 7, the slot is to be placed between the first and second spans (r=5.5m and 11m) with 5.5m length, where the separation is present.

The slot width has to be minimized while preserving its performance in removing the stalled boundary layer. Narrow passages cannot extract enough fluid to reattach the flow, while large passages need much more energy and can affect the main flow and disturb expected airfoil performance. The optimal width can be found by simulating the suction system.

To simulate the performance of the suction slot, a new boundary condition has to be defined on some regions of the blade surface. Considering the time required to modify the 3D model and regenerate a grid, for the study of different slot width, a shortcut solution has been implemented in this work. To resolve this issue, a code has been developed. This code, obtains the original grid of the domain as an input file. It then recognizes the file data structure and identifies the blade surface nodes.

Nodes located inside the desired slot region have been extracted and redefined as a new surface and boundary at the end of the file (Fig. 11). Finally, the file has been reassembled and prepared to be read by the flow solver. In this work, several slot widths have been considered and finally 3cm is suggested. This size presented the best performance with the lowest mass flow and energy consumption.

5. RECTIFIED FLOW FIELD

After setting the slot size and location, its mass flow rate is the last remaining parameter. Since no data were readily available for it, some values were selected and blade performance was simulated for each as depicted in Fig. 12. Here three most important result sets are presented. The lowest suction intensity is 0.5kg/s which can improve the power coefficient by up to 0.04 point equivalent to 8% at TSR=7. The minimum improvement occurs at TSR=9 being equal to 0.015 point or 3.1%. By doubling the suction mass flow rate, slightly better performance can be achieved by increasing the power coefficient by another 0.01 point. At this point, further increase in suction intensity worsens the performance as shown in the plot. Thus, it can be concluded that the optimum suction mass flow rate is about 1kg/s. However, taking into account the energy required for doubling the

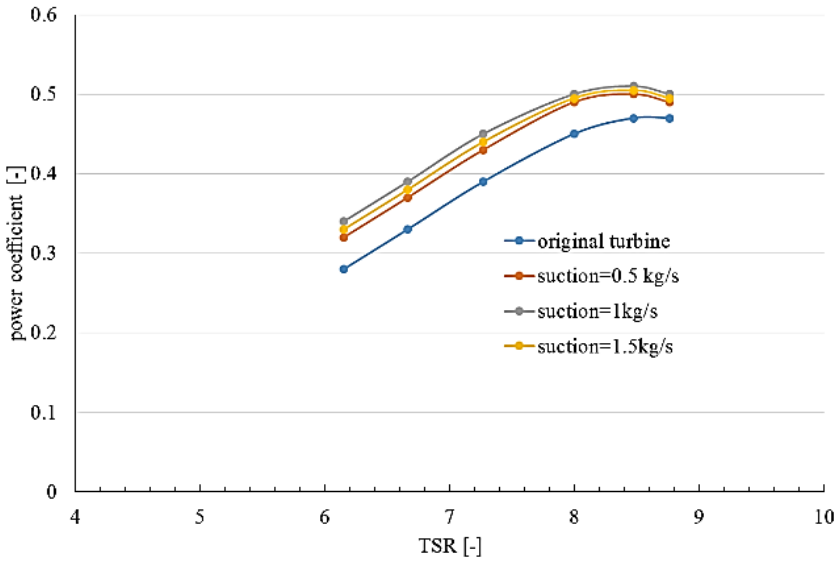

Fig. 11 Effect of suction mass flow rate on power coefficient

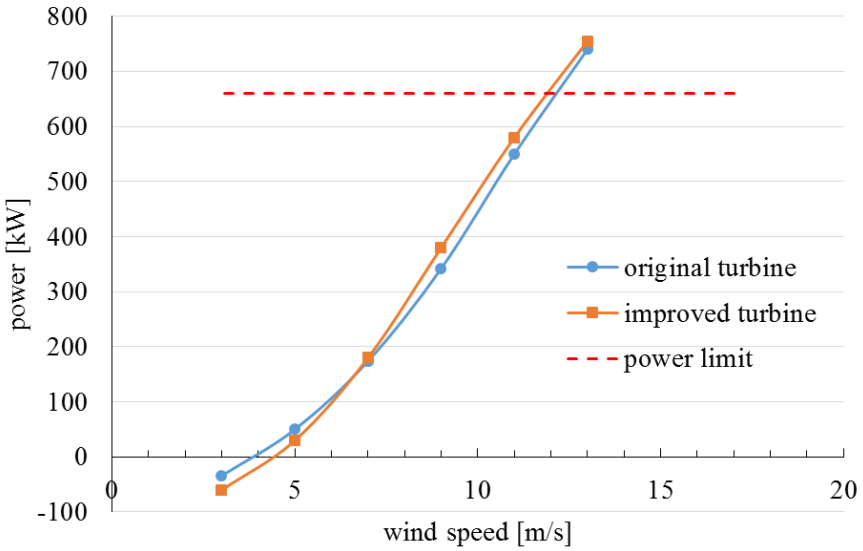

Fig. 12 Power curve of the turbine with different configurations

mass flow rate and comparatively small performance gain, it would be wise to select 0.5kg/s as the best choice.

To better estimate the performance improvement, we need to take a look at the power curve which exactly depicts the turbine output (Fig. 13). It can be observed that the suction system is not beneficial at low wind speeds below 6m/s. According to Fig.5, this range corresponds to high TSR (region I) where the angle of attack is low and no separation is expected. Applying suction at this condition (where no separation exists) disturbs the correct airfoil pressure profile on the suction side and lowers the lift coefficient. At wind speeds above 7m/s, the changes are positive leading to higher shaft power. The maximum power increase is about 38kW at wind speed of 9m/s. At higher wind speeds the turbine reaches its maximum possible power production (red dash line), at which the pitch system starts to reduce the blade loading. Hence, the suction system is no more needed. This can be easily accomplished by turning off the suction fan.

To emphasize the root cause of performance improvement, the same streamlines of Fig.7 at TSR=7 with and without the suction of 0.5kg/s are illustrated in Fig. 14. It can be easily observed that the separation point is pushed back from 0.55 chord length to 0.90 by the suction system.

6. IMPLEMENTATION METHOD

Practically, some issues have to be resolved to render the system applicable. First, a route should be defined for the suctioned air flow. Having in mind that the blade has a shell and hollow structure, it can be itself considered as a duct.

Thus, the extracted fluid can be transferred through the blade and reach the hub. This suction can be performed by a simple fan at the root interface.

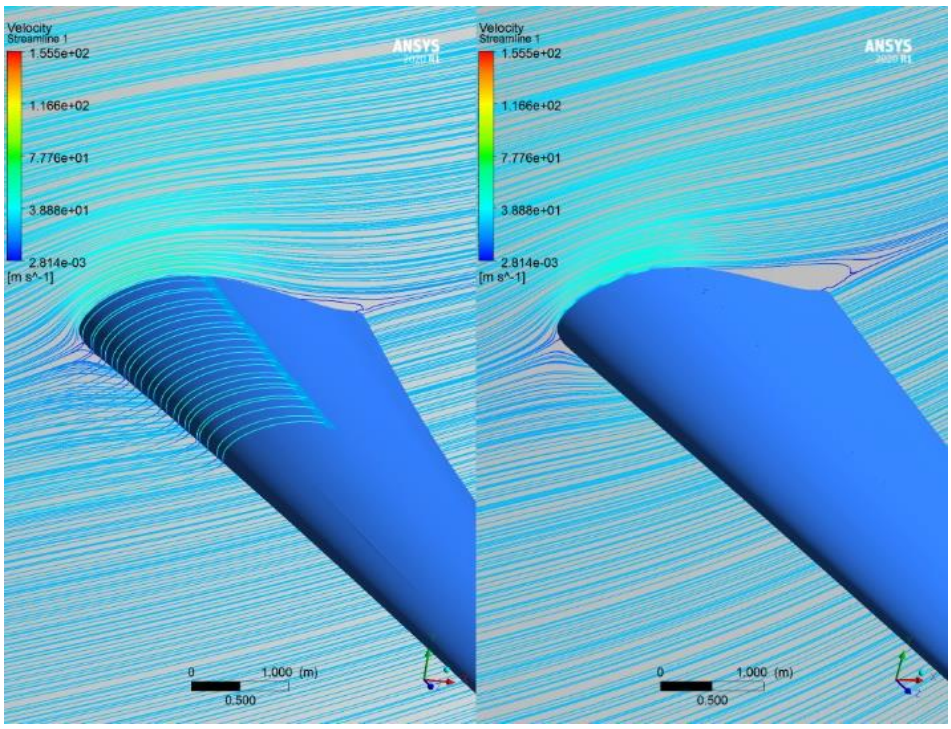

Fig. 13 Streamlines with (left) and without (right) suction

Fig. 14 Blade root geometry

Wind turbine blades have a manhole inside the root section which is required for inspections (Fig.15). Here it is suggested to remove the opening and install a simple axial fan there. Blades are connected to the hub. The flange connection is fully open so suctioned air can be collected inside the hub. The hub itself has many holes and openings inside, used for transferring the equipment and wires. Therefore, air can be exhausted into the atmosphere quite easily.

The second issue is the power required for fans and their technical specifications. Here at nominal conditions, the pressure difference at the slot is about 800Pa.

The pressure difference generated by centrifugal force of air inside the blade for a radius of 11m, density of 1.225 kg/m^3 and omega=2.93 rad/s is about 633Pa. Further, the mass flow rate of 1kg/s is equivalent to 0.83m^3/s or 2990m^3/h. This is very normal for a regular fan and easily available on the market. Such a fan has a power consumption of about 1500W which is well below the power gained from aerodynamic corrections.

Finally, the control strategy has to be determined. As shown earlier, the suction system does not lead to a power increase at wind speeds below 7m/s. Also, at wind speeds higher than 12m/s, the turbine power is higher than required. In other words, the suction system should be turned on, within a certain wind speed range. This constraint can be easily defined in the central control system. It should be stated that a simple on/off strategy is enough for this application and it is not required to continuously control and adjust the suction intensity.

7. CONCLUSION

This research demonstrated that the fixed geometry of wind turbine blades, coupled with generator limitations in regulating rotor speed, can drive the blades into off-design operating conditions, resulting in suboptimal aerodynamic performance. CFD simulations on a commercial wind turbine revealed that this undesired operating range is characterized by flow separation at the inboard section of the blades.

To address this issue, the implementation of a boundary layer suction system was investigated. Considering structural constraints, a slot was incorporated into the blade surface, and the turbine performance was re-evaluated with this new configuration. Main findings can be listed as below:

1- Simulations showed that applying appropriate suction intensity could enhance the aerodynamic power coefficient by up to 8% in certain situations.

2- It is observed that the suction system effectively minimized flow separation (though not entirely

eliminating it), promoting an attached streamline and consequently improving lift and reducing section drag.

3- The suction system proved beneficial only within a limited wind speed range of 6-12 m/s and required deactivation outside this range.

CONFLICT OF INTEREST

The authors declare that they have no known competing financial interests or personal relationships that could have appeared to influence the work reported in this paper.

AUTHORS CONTRIBUTION

S. Sadi: Methodology, Writing Conceptualization, original draft, Literature survey. **M. R. Asayesh**: Conceptualization, Methodology, Software, Validation, Data Curation, Visualization, Formal analysis, Investigation, Writing original draft. **S. A. Moussavi**: Conceptualization, Supervision, Methodology, Software, Writing review & editing.

REFERENCES

Alfrefai, M., & Acharya, M. (1996). Controlled leading-edge suction for management of unsteady separation pitching airfoils. *AIAA 1995-2188. Fluid Dynamics Conference.* https://doi.org/10.2514/6.1995-2188.

Arnold B., Lutz T., Kramer E. (2018). Design of a boundary layer suction system for turbulent trailing edge noise reduction of wind turbines. *Journal of Renewable Energies*, (123), 249-262. https://doi.org/10.1016/j.renene.2018.02.050

Basualdo, S. (2005). Load alleviation on wind turbine blades using variable geometry. *Wind Engineering, 29* (2), 169-182. https://doi.org/10.1260/0309524054797122

Barlas, T. K., & Van Kuik, G. A. M. (2007, July). *State of the art and prospectives of smart rotor control for wind turbines.* Journal of Physics: Conference Series. IOP Publishing. https://doi.org/10.1088/1742-6596/75/1/012080

Griffin, D. (1996). *Investigation of vortex generators for augmentation of wind turbine power performance*. NREL, USA.

Guoqiang, L., & Shihe, Y. (2020). Large eddy simulation of dynamic stall flow control for wind turbine airfoil using plasma actuator. *Energy,* (212), 15084. https://doi.org/10.1016/j.energy.2020.118753

Huang, S., Qiu, H., & Wang, Y. (2023). Numerical study of aerodynamic performance of airfoil with variable curvature split flap. *Journal of Applied Fluid Mechanics*, *16*(6), 1108-1118. https://doi.org/10.47176/jafm.16.06.1531

Jacob, J., & Santhanakrishnan, A. (2005). *Effect of regular surface perturbations on flow over an airfoil*. 35th AIAA Fluid Dynamics Conference and Exhibit. https://doi.org/10.2514/6.2005-5145

Jukes, T. N. (2015). Smart control of a horizontal axis wind turbine using dielectric barrier discharge plasma actuators. *Renewable Energy*, (80), 644-654. https://doi.org/10.1016/j.renene.2015.02.047

Karim, M. A., & Acharya, M. (1994). Suppression of dynamic stall vortices over pitching airfoils by leading-edge suction. *AIAA Journal, 32*, 1647-1655. https://doi.org/10.2514/3.12155

Ma, C. Y., & Xu, H. Y. (2023). Parameter-based design and analysis of wind turbine airfoils with conformal slot co-flow jet. *Journal of Applied Fluid Mechanics*, *16*(2), 269-283. https://doi.org/10.47176/jafm.16.02.1318

Maali Amiri, M. M., Shadman, M., & Estefen, S. F. (2020). URANS simulations of a horizontal axis wind turbine under stall condition using Reynolds stress turbulence models. *Energy*, *213*, 118766. https://doi.org/10.1016/j.energy.2020.118766

Mahboub, A., Bouzit, M., & Ghenaim, A. (2022). Effect of different shaped cavities and bumps on flow structure and wing performance. *Journal of Applied Fluid Mechanics*, *15*(6), 1649-1660. https://doi.org/10.47176/jafm.15.06.1108

Mayda, E. A., & van Dam, C. P. (2005). *Computational investigation of finite width microtabs for aerodynamic load control.* 35th AIAA Fluid Dynamics Conference and Exhibit. https://doi.org/10.2514/6.2005-1185

Mereu, R., Passoni, S., & Inzoli, F. (2019). Scale-resolving CFD modeling of a thick wind turbine airfoil with application of vortex generators: Validation and sensitivity analyses. *Energy*, (187), 115969. https://doi.org/10.1016/j.energy.2019.115969

Moussavi, S. A. & Ghaznavi, A. (2021). Effect of boundary layer suction on performance of a 2 MW wind turbine, *Journal of Energy* (232), 121072. https://doi.org/10.1016/j.energy.2021.121072

Ozkan, M., & Erkan, O. (2022). Control of a boundary layer over a wind turbine blade using distributed passive roughness. *Journal of Renewable Energy* (184), 421-429. https://doi.org/10.1016/j.renene.2021.11.082

Pechlivanoglou, G. (2013). *Passive and active flow control solutions for wind turbine blades* [PhD dissertation], TU berlin, Germany. https://doi.org/10.14279/depositonce-3487

Pechlivanoglou, G., Wagner, J., Nayeri, C., & Paschereit, C. (2010, January). *Active aerodynamic control of wind turbine blades with high deflection flexible flaps.* 48th AIAA Aerospace Sciences Meeting Including the New Horizons Forum and Aerospace Exposition. https://doi.org/10.2514/6.2010-644

Rezaeiha, A., Montazeri, H., & Blocken, B. (2019). On the accuracy of turbulence models for CFD simulations

of vertical axis wind turbines. *Energy*, *180*, 83857. https://doi.org/10.1016/j.energy.2019.05.053

Sedighi, H., Akbarzadeh, P., & Salavatipour, A. (2020). Aerodynamic performance enhancement of horizontal axis wind turbines by dimples on blades: Numerical investigation. *Energy*, (195), 17056. https://doi.org/10.1016/j.energy.2020.117056

Shi, X., Xu, S., & Huang, D. (2019). Passive flow control of a stalled airfoil using an oscillating micro-cylinder. *Computers & Fluids*, (178), 152-165. https://doi.org/10.1016/j.compfluid.2018.08.012

Spera, D. (2009). *Wind Turbine Technology.* ASME.

Supreeth, R., Arokkiaswamy, A., Anirudh, K., Pradyumna, R. K., Pramod, P. K., and Sanarahamat, A. K. (2020). Experimental and numerical investigation of the influence of leading edge tubercles on S823 airfoil behavior. *Journal of Applied Fluid Mechanics*, *13*(6), 1885-1899. https://doi.org/10.47176/jafm.13.06.31244

Van Wingerden, J. W., Hulskamp, A. W., Barlas, T., Marrant, B., Van Kuik, G. A. M., Molenaar, D. P., & Verhaegen, M. (2008). On the proof of concept of a 'smart'wind turbine rotor blade for load alleviation. *Wind Energy: An International Journal for Progress and Applications in Wind Power Conversion Technology*, *11*(3), 265-280. https://doi.org/10.1002/we.264

Wang, S. C. (1995). *Control of dynamic stall* [PhD Dissertation, Florida State University], Mechanical Engineering Department, USA.

Yousefi, K., Saleh, S. R., & Zahedi, P. (2013). Numerical investigation of suction and length of suction jet on aerodynamic characteristics of the NACA 0012 airfoil. *International Journal of Materials, Mechanics and Manufacturing*, *1* (2), 136-142. https://doi.org/10.7763/IJMMM.2013.V1.30

Zhu, C., Chen, J., Wu, J., & Wang, T. (2019). Dynamic stall control of the wind turbine airfoil via single-row and double-row passive vortex generators. *Energy*, (189), 11627. https://doi.org/10.1016/j.energy.2019.116272